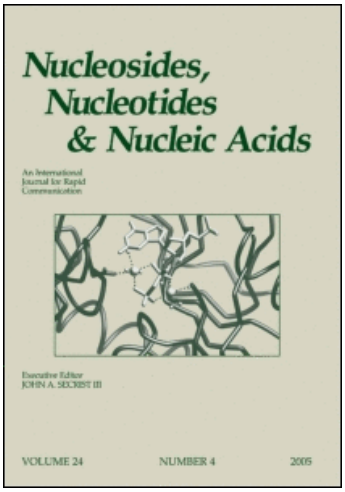

Nucleosides, Nucleotides and Nucleic Acids
Publication details, including instructions for authors and subscription information:
http://www.informaworld.com/smpp/title~content=t713597286

Hydrolytic Stability of a Phosphate-Branched Oligonucleotide Incorporating a Ribonucleoside 3'-Phosphotriester Unit

Tuomas Lönnberg[a]
[a] Department of Chemistry, University of Turku, Turku, Finland

To cite this Article Lönnberg, Tuomas(2006) 'Hydrolytic Stability of a Phosphate-Branched Oligonucleotide Incorporating a Ribonucleoside 3'-Phosphotriester Unit', Nucleosides, Nucleotides and Nucleic Acids, 25: 3, 315 — 323
To link to this Article: DOI: 10.1080/15257770500544537
URL: http://dx.doi.org/10.1080/15257770500544537

Nucleosides, Nucleotides, and Nucleic Acids, 25:315–323, 2006

ISSN: 1525-7770 print / 1532-2335 online
DOI: 10.1080/15257770500544537

Taylor & Francis
Taylor & Francis Group

HYDROLYTIC STABILITY OF A PHOSPHATE-BRANCHED OLIGONUCLEOTIDE INCORPORATING A RIBONUCLEOSIDE 3′-PHOSPHOTRIESTER UNIT

Tuomas Lönnberg □ *Department of Chemistry, University of Turku, Turku, Finland*

□ *A phosphate-branched oligonucleotide has been prepared by using an appropriately protected trinucleoside phosphotriester building block in conventional solid-phase synthesis. Hydrolysis of the branched oligonucleotide has been followed over a wide pH range. Comparison of the present results with those previously obtained for simpler analogues indicates that a trinucleoside 3′,3′,5′-monophosphate, when embedded in an oligonucleotide structure, is stabilized toward hydroxide-ion catalyzed cleavage by more than one order of magnitude, lending some support to the feasibility of existence of phosphate-branched RNA X in biological systems.*

Keywords RNA; Hydrolysis; Mechanism; Phosphate-Branched Oligonucleotide; RNA X

INTRODUCTION

A branched RNAstructure containing a phosphotriester linkage, the so-called RNA X (Figure 1), has been suggested to be formed in the catalytic domain of human spliceosome.[1,2] The two residues flanking the proposed phosphotriester linkage, viz. A53 and G54, are 2′-O-methylated,[3] which greatly increases the stability of the phosphotriester toward hydrolysis. On the basis of our previous studies,[4,5] methylation of the free 2′-OH in a trinucleoside 3′,3′,5′-monophosphate mimic of RNA X, 2′,3′-*O*-methyleneadenosin-5′-yl 2′,5′-di-*O*-methyluridin-3′-yl 5′-*O*-methyluridin-3′-yl phosphate (**1**), increases the hydrolytic stability by at least three orders of magnitude, resulting in a half-life of more than one day under physiological conditions. However, the original observations on the existence of RNA X also referred to in vitro transcribed snRNAs composed entirely of the four native ribonucleosides[1,2] and such triester structures do not experience

Received 23 August 2005; accepted 29 December 2005.
The assistance of Dr. Petri Heinonen and Päivi Poijärvi with the oligonucleotide synthesis is gratefully recognized.
Address correspondence to Tuomas Lönnberg, Department of Chemistry, University of Turku, Vatselankatu 2, FIN-20014 Turku, Finland. E-mail: tuanlo@utu.fi

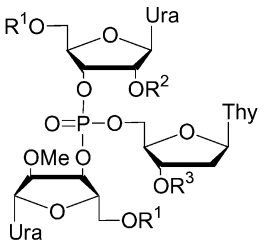

2a: $R^1 = (Tp)_3, R^2 = H, R^3 = (pT)_6$
2b: $R^1 = DMTr, R^2 = Lev,$
$R^3 = TBDMS$
2c: $R^1 = DMTr, R^2 = Lev,$
$R^3 = P(N^iPr_2)OCH_2CH_2CN$
2d: $R^1 = (Tp)_3, R^2 = Lev, R^3 = (pT)_6$
2e: R^1 =DMTr, R^2 = Lev, R^3 = H

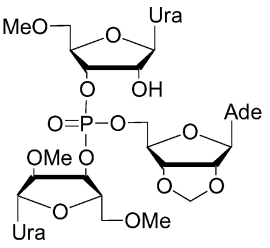

1

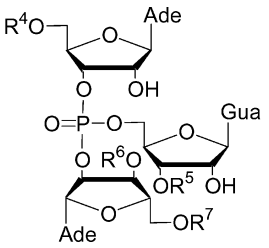

RNA X

R^4 = 5′-terminal sequence of U6
R^5 = 3′-terminal sequence of U6
R^6 = 3′-terminal sequence of Br
R^7 = 5′-terminal sequence of Br

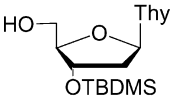

3

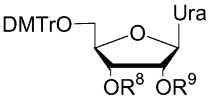

4: $R^8 = H, R^9 = Me$
5a: $R^8 = H, R^9 = Lev$
5b: $R^8 = Lev, R^9 = H$

FIGURE 1 Structures of the branched building blocks and oligonucleotides **2a-e**, their constituent protected nucleosides **3-5**, the trinucleoside monophosphate **1**, and RNA X.

a similar stabilization by 2′-*O*-alkylation. The results obtained with the trinucleoside 3′,3′,5′-monophosphate model (**1**), when extrapolated to physiological conditions, suggest a half-life of only 100 s for phosphate-branched RNA,[4] hardly supporting the existence of the proposed species. It is, however, possible that in the actual RNA X the flanking oligonucleotide strands stabilize the phosphotriester linkage by causing a conformational change that retards the in-line displacement of the 2′- or 5′-linked nucleoside or by altering the solvation of the initial and/or transition state.[6,7] To elucidate whether **1** could really be expected to experience a marked stabilization when embedded in an oligonucleotide structure, a small phosphate-branched oligonucleotide (**2a**) has been synthesized and its hydrolytic reactions have been followed over a wide pH range. Since the oligonucleotide arms consist solely of thymidine residues (Figure 1), they are not expected to have any specific interactions with each other. Any changes in reactivity should, hence, be due to steric or electrostatic repulsion between the oligonucleotide strands and changes in solvation of the initial and/or transition state compared to **1**.

EXPERIMENTAL

Oligonucleotide Sythesis

An appropriately protected trinucleoside phosphotriester (**2b**) was first synthesized as previously described, viz. by tetrazole-promoted stepwise displacement of the dimethylamino groups from tris(dimethylamino)-phosphine with the appropriately protected nucleosides, added in the order: (1) 3′-*O*-(*tert*-butyldimethylsilyl)thymidine, (2) 5′-*O*-(4,4′-dimethoxytrityl)-2′-*O*-methyluridine, (3) 5′-*O*-(4,4′-dimethoxytrityl)-2′-*O*-levulinyluridine.[3,5,8] The TBDMS protection was removed and the exposed 3′-hydroxy function was phosphitylated to yield **2c**. The oligonucleotide was then assembled on a CPG-supported Q-linker at a loading of 28 μmol g^{-1} (Scheme 1). Standard phosphoramidite strategy was utilized, except that a prolonged coupling time (600 s) was applied to the branching building block **2c**. The coupling efficiency of the branching unit was 72%. The subsequent elongation of the two 5′-branches then proceeded by normal efficiency. After completion of the chain assembly, the cyanoethyl groups were removed by 3 min treatment

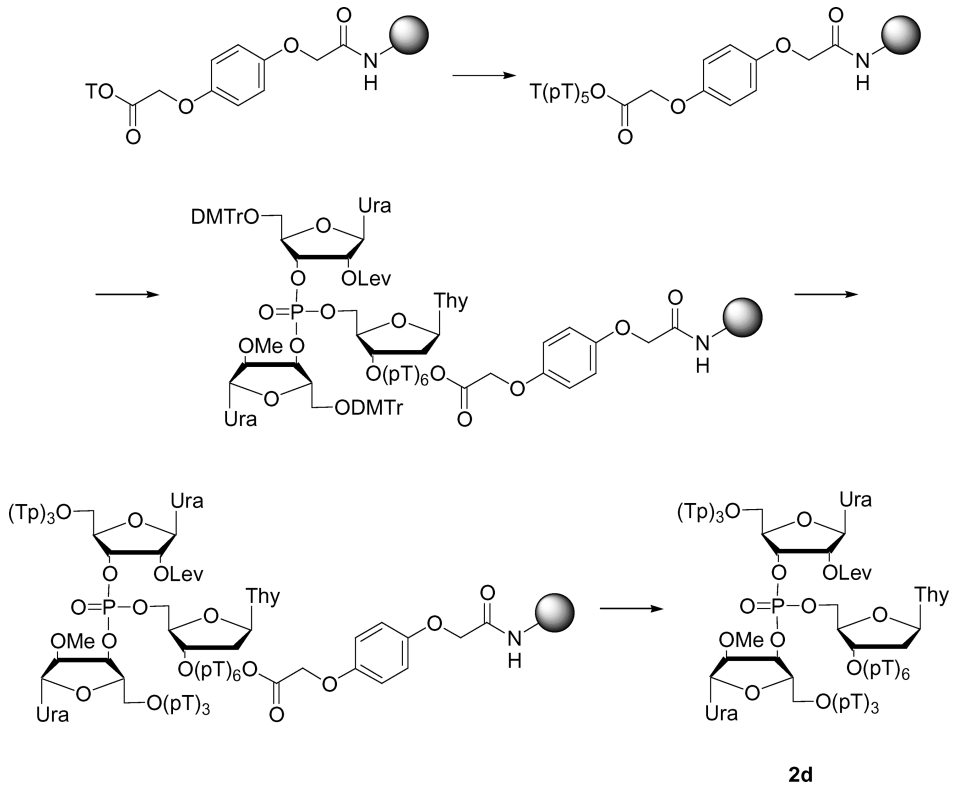

SCHEME 1 Synthesis of the protected branched oligonucleotide **2d**.

with 1.5% (v/v) DBU in MeCN and the linker was cleaved by 1 min treatment with 50 mmol L^{-1} methanolic K_2CO_3. Finally, the released product **2d** was purified by RP HPLC and characterized by ESI-MS.

Kinetics of the Hydrolysis of 2a

Because **2a** is an unstable compound, the 2′-levulinyl protection of **2d** has to be removed immediately before each kinetic run. The deprotection conditions were optimized by using 2′-*O*-levulinyluridine as a model compound. In a mixture of hydrazine, acetic acid, and DMSO (1:7:404, v/v) at 25°C, total conversion of 2′-*O*-levulinyluridine to uridine was achieved in 15 min. The hydrolysis of **2a** was followed over a wide pH range (0–9) at 25°C and a constant ionic strength of 1.0 mol L^{-1} ($NaNO_3$) by analyzing the composition of the aliquots withdrawn from the reaction mixture at appropriate time intervals by capillary electrophoresis. Prior to each kinetic run, the 2′-*O*-levulinyl group of **2d** was removed by 20-min treatment with hydrazinium acetate in DMSO, as described above, to yield **2a**. The deprotection reaction was then quenched with acetone and the appropriate aqueous solution was created in the reaction vessel so that the final amounts of DMSO and acetone were 3% and 1% (v/v), respectively. The aliquots withdrawn were, in turn, quenched by cooling to 0°C and adjusting their pH to approximately 3 with a citric acid buffer.

3′-*O*-(*tert*-Butyldimethylsilyl)thymidine (3). The compound was prepared by using established synthetic procedures.[1] ^{1}H NMR (δ_H) (500 MHz, DMSO-d_6) 11.30 (s, 1H), 7.67 (s, 1H), 6.15 (dd, $J_1 = 6.9$ Hz, $J_2 = 7.0$ Hz), 5.08 (s, 1H), 4.14 (m, 1H), 3.76 (m, 1H), 3.57 (m, 2H), 2.19 (m, 1H), 2.04 (m, 1H), 1.77 (s, 3H), 0.88 (s, 9H), 0.09 (s, 6H). HRMS (FAB) M^+ calcd 357.1855, obsd 357.1846.

5′-*O*-(4,4′-Dimethoxytrityl)-2′-*O*-methyluridine (4). 2′-*O*-Methyluridine was prepared as desribed in the literature,[9] after which the 5′-*O*-dimethoxytrityl protection was attached by the conventional method. ^{1}H NMR (δ_H) (500 MHz, DMSO-d_6) 11.42 (s, 1H), 7.74 (d, 1H, $J = 8.1$ Hz), 7.39–7.14 (m, 13H), 5.30 (d, 1H, $J = 8.1$ Hz), 5.24 (d, 1H, $J = 7.0$ Hz), 4.21 (m, 1H), 3.95 (m, 1H), 3.82 (m, 1H), 3.75 (s, 6H), 3.42 (s, 3H), 3.29–3.23 (m, 2H). ESI^--MS m/z 559.1 $[M\text{-}H]^-$.

5′-*O*-(4,4′-Dimethoxytrityl)-2′(3′)-*O*-levulinyluridine (5a,b). 5′-O-(4,4′-Dimethoxytrityl)uridine (10.8 mmol, 5.87 g) was dissolved in pyridine (50 mL). A solution of levulinic anhydride (11.9 mmol, 2.54 g) in 1,4-dioxane (50 mL) was added, followed by a catalytic amount of DMAP. After stirring for 4 h at room temperature, the reaction mixture was evaporated to dryness

and a conventional aq. $NaHCO_3/CH_2Cl_2$ was carried out. The organic phase was evaporated to dryness and the residue was purified on a silica gel column eluting with a mixture of Et_3N, MeOH, and CH_2Cl_2 (1:4:95, v/v). The product was obtained as a mixture of **5a** and **5b** (2:1) in an overall yield of 78% (5.41 g). ^1H NMR (δ_H) (500 MHz, DMSO-d_6, **5a**) 11.43 (s, 1H), 7.69 (d, 1H, $J = 8.1$ Hz), 7.41–7.23 (m, 13H), 5.81 (d, 1H, $J = 5.9$ Hz), 5.78 (d, 1H, $J = 5.8$ Hz), 5.45 (d, 1H, $J = 8.1$ Hz), 5.14 (m, 1H), 4.41 (m, 1H), 4.10 (m, 1H), 3.75 (s, 6H), 3.34–3.19 (m, 2H), 2.74 (m, 2H), 2.55 (m, 2H), 2.11 (s, 3H). ^1H NMR (δ_H) (500 MHz, DMSO-d_6, **5b**) 11.43 (s, 1H), 7.67 (d, 1H, $J = 8.1$ Hz), 7.41–7.23 (m, 13H), 5.91 (d, 1H, $J = 5.7$ Hz), 5.55 (d, 1H, $J = 5.8$ Hz), 5.42 (d, 1H, $J = 8.1$ Hz), 5.26 (m, 1H), 4.35 (m, 1H), 3.99 (m, 1H), 3.75 (s, 6H), 3.34–3.19 (m, 2H), 2.74 (m, 2H), 2.55 (m, 2H), 2.11 (s, 3H). HRMS (FAB) M^- calcd 643.2314, obsd 643.2292.

3′-*O*-(*tert*-Butyldimethylsilyl)thymidin-5′-yl 5′-*O*-(4,4′-dimethoxytrityl)-2′-*O*-methyluridin-3′-yl 5′-*O*-(4,4′-dimethoxytrityl)-2′-*O*-levulinyluridin-3′-yl phosphate (2b). 3′-*O*-(*tert*-Butyldimethylsilyl)thymidine (**3**, 4.95 mmol, 1.77 g) was dissolved in anhydrous MeCN (5 mL) and tris(dimethylamino)phosphine (5.11 mmol, 0.928 mL) and 1H-tetrazole (5.94 mmol, 0.416 g) in anhydrous MeCN (13.2 mL) were added. After stirring for 1 h at room temperature under inert atmosphere, 5′-*O*-methyl-(4,4′-dimethoxytrityl)-2′-*O*-methyluridine (**4**, 4.95 mmol, 2.78 g) and 1H-tetrazole (5.94 mmol, 0.416 g) in anhydrous MeCN (13.2 mL) were added. The reaction mixture was stirred for 22 h, after which 5′-*O*-(4,4′-dimethoxytrityl)-2′(3′)-*O*-levulinyluridine (**5a**,**b**, 8.39 mmol, 5.41 g) and 1H-tetrazole (5.94 mmol, 0.416 g) in anhydrous MeCN (13.2 mL) were added. After stirring for 24 h, iodine (5.50 mmol, 1.41 g) in a mixture of water (8.6 mL), THF (17.2 mL), and 2,6-lutidine (4.3 mL) was added. The reaction mixture was stirred for 1 h, after which it was concentrated under reduced pressure. The residue was dissolved in CH_2Cl_2 and washed with saturated aqueous $NaHSO_3$. The aqueous phase was back-extracted with CH_2Cl_2. The combined organic phases were evaporated to dryness and the residue was purified on a silica gel column eluting first with a mixture of Et_3N, MeOH, and CH_2Cl_2 (1:6:93, v/v), then with a mixture of Et_3N, MeOH, CH_2Cl_2, and EtOAc (1:3:18:78, v/v). Yield 34.5% (1.81 g). ^1H NMR (δ_H) (500 MHz, DMSO-d_6) 11.48 (s, 1H), 11.45 (s, 1H), 11.33 (s, 1H), 7.66 (d, 1H, $J = 8.1$ Hz), 7.61 (d, 1H, $J = 8.1$ Hz), 7.43 (s, 1H), 7.41–7.19 (m, 26H), 6.17 (dd, 1H, $J_1 = 6.9$ Hz, $J_2 = 7.0$ Hz), 5.92 (d, 1H, $J = 5.5$ Hz), 5.73 (d, 1H, $J = 3.0$ Hz), 5.50 (dd, 1H, $J_1 = 8.1$ Hz, $J_2 = 1.4$ Hz), 5.39 (dd, 1H, $J_1 = 8.1$ Hz, $J_2 = 1.6$ Hz), 5.35 (m, 1H), 5.16 (m, 1H), 5.07 (m, 1H), 4.38 (m, 1H), 4.29 (m, 1H), 4.21–4.11 (m, 4H), 3.95 (m, 1H), 3.74 (s, 6H), 3.71 (s, 6H), 3.40 (s, 3H), 3.39–3.24 (m, 4H), 2.75–2.55 (m, 4H), 2.22 (m, 1H), 2.07 (m, 1H), 2.05 (s, 3H), 1.71 (s, 3H), 0.85 (s, 9H), 0.07 (s, 3H), 0.06 (s, 3H). ^{31}P NMR

(δ_P) (202 MHz, DMSO-d_6) −2.46. HRMS (FAB) M^- calcd 1603.5589, obsd 1603.5670.

Thymidin-5′-yl 5′-*O*-(4,4′-dimethoxytrityl)-2′*O*-methyluridin-3′-yl 5′-*O*-(4,4′-dimethoxytrityl)-2′-*O*-levulinyluridin-3′-yl phosphate (2e). 3′-*O*-(*tert*-Butyldimethylsilyl)thymidin-5′-yl 5′-*O*-(4,4′-dimethoxytrityl)-2′-*O*-methyluridin-3′-yl 5′-*O*-(4,4′-dimethoxytrityl)-2′-*O*-levulinyluridin-3′-yl phosphate (**2b**, 0.458 mmol, 0.735 g) was dissolved in THF (3.14 mL) and $Et_3N{\cdot}3HF$ (112 μL) was added. After being stirred for 18 h at room temperature, the reaction mixture was purified on a silica gel column eluting with a mixture of Et_3N, MeOH, and CH_2Cl_2 (1:6:93, v/v). Yield 65.7% (0.449 g). ^1H NMR (δ_H) (500 MHz, DMSO-d_6) 11.45 (m, 2H), 11.33 (s, 1H), 7.67 (d, 1H, J = 8.1 Hz), 7.60 (d, 1H, J = 8.1 Hz), 7.39 (s, 1H), 7.37–7.19 (m, 26 H), 6.18 (dd, 1H, J_1 = 6.9 Hz, J_2 = 7.0 Hz), 5.89 (d, 1H, J = 5.5 Hz), 5.72 (d, 1H, J = 3.0 Hz), 5.47 (d, 1H, J = 8.1 Hz), 5.36 (d, 1H, J = 8.1 Hz), 5.35 (m, 1H), 5.26 (m, 1H), 5.15 (m, 1H), 4.28 (m, 2H), 4.25–4.08 (m, 4H), 3.93 (m, 1H), 3.74 (s, 6H), 3.70 (s, 6H), 3.38 (s, 3H), 3.37–3.22 (m, 4H), 2.75–2.55 (m, 4H), 2.45 (m, 2H), 2.05 (s, 3H), 1.70 (s, 3H). MS (FAB) M^- calcd 1489.5, obsd 1490.

***O*^{P}-[5′-*O*-(4,4′-Dimethoxytrityl)-2′-*O*-methyluridin-3′-yl]-[5′-*O*-(4,4′-dimethoxytrityl)-2′-*O*-levulinyluridylyl-(3′,5′)-thymidine] 3′-(2-cyanoethyl-*N*,*N*-diisopropylphosphoramidite) (2c).** Thymidin-5′-yl 5′-*O*-(4,4′-dimethoxytrityl)-2′-*O*-methyluridin-3′-yl 5′-*O*-(4,4′-dimethoxytrityl)-2′-*O*-levulinyluridin-3′-yl phosphate (**2e**, 0.259 mmol, 0.449 g) was dissolved in anhydrous MeCN (11 mL) and 2-cyanoethyl-*N*,*N*,*N*′,*N*′-tetraisopropylphosphorodiamidite (0.472 mmol, 150 μL) and 1H-tetrazole (0.36 mmol, 0.0252 g) in anhydrous MeCN (800 μL) were added. The reaction mixture was stirred for 17 h at room temperature, after which CH_2Cl_2 (50 mL) and 5% (m/m) aqueous $NaHCO_3$ (30 mL) were added. The phases were separated and the organic phase was dried (Na_2SO_4) and evaporated to dryness. On the basis of the ^{31}P NMR spectrum the yield was estimated to be 76%. ^{31}P NMR (δ_P) (202 MHz, DMSO-d_6) −148.15 (s, 1P), −2.47 (s, 1P). HRMS (FAB) M^- calcd 1689.5835, obsd 1689.5884.

RESULTS AND DISCUSSION

At pH < 6, disappearance of the starting material is accompanied by formation of four product peaks at approximately 2:1:2:2 ratio. At pH > 6, only the peaks of the two faster migrating products are observed at approximately 2:1 ratio. Previous studies with trinucleoside 3′,3′,5′-monophosphates have revealed a similar change in product distribution: under acidic conditions, the P-O3′ and P-O5′ bonds are cleaved at approximately equal rates, whereas

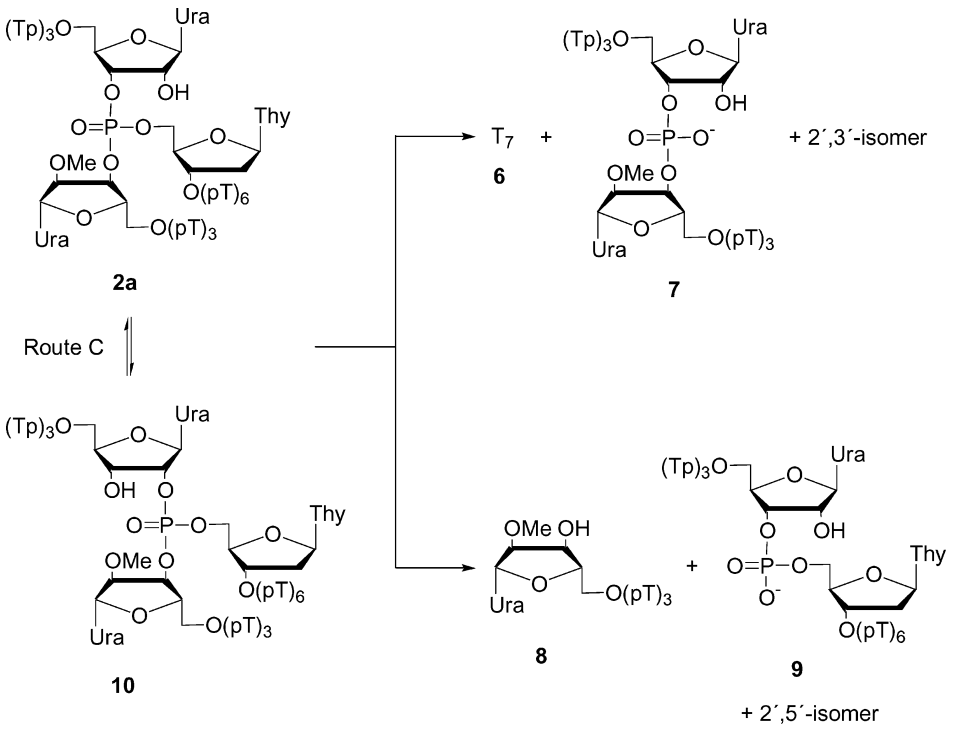

SCHEME 2 Hydrolytic reaction pathways of the branched oligonucleotide **2a**.

in aquous alkali the P-O3′ bond cleavage accounts for almost 90% of the overall reaction.[3,8] Assuming that hypochromicity is negligible, the potential product oligonucleotides **6**, **7**, **8,** and **9** (Scheme 2) should have relative molar absorptivities of 7, 8, 4, and 11, respectively. Accordingly, the faster migrating pair of product peaks was assigned as **9** and **8**, respectively, and the slower migrating pair as **6** and **7**, respectively. Mass spectrometric analysis of reaction solutions lacking the background electrolyte tends to support this interpretation. Accordingly, in 10 mmol L^{-1} HNO_3, the following ions were observed (m/z): **2a**: 887.0 (M^{5-}), 738.8 (M^{6-}); **6**: 1032.8 (M^{2-}), 688.4 (M^{3-}), 412.4 (M^{5-}); **7**: 1194.5 (M^{2-}), 596.6 (M^{4-}), 396.2 (M^{6-}), 340.1 (M^{7-}); **8**: 584.3 (M^{2-}), 389.9 (M^{3-}); **9**: 1164.2 (M^{2-}), 468.2 (M^{7-}). In 10 mmol L^{-1} NaOH, **2a** is decomposed within seconds and only product ions were, hence, detected (m/z): **8**: 389.9 (M^{3-}), **9**: 547.1 (M^{6-}). Undoubtedly, **2a** also undergoes a facile isomerization to its 2′,3′,5′-analogue **10** (Scheme 1, Route C), although only one peak corresponding to starting material is observed. Apparently the two isomers migrate equally rapidly, hence preventing their separation by capillary electrophoresis.

The pH-rate profile for the disappearance of **2a** is depicted in Figure 2. At pH < 2, the overall disappearance of **2a** is first-order in [H_3O^+]. On the basis of the observed product ratio (2:1:2:2) and relative molar absorptivities

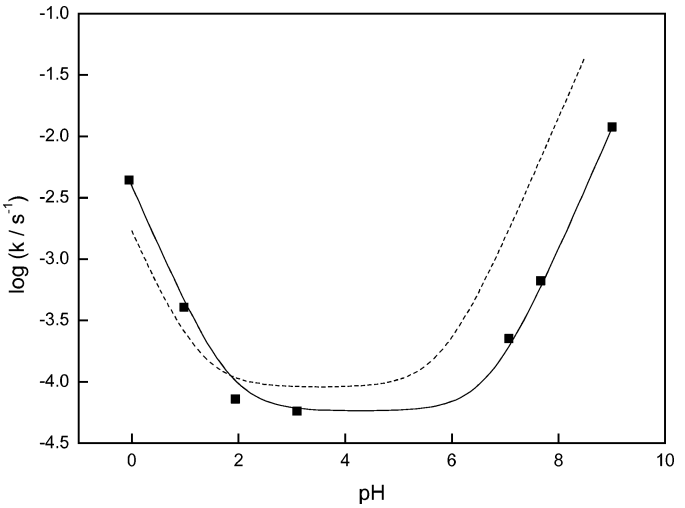

FIGURE 2 pH-Rate profiles for the cleavage of the branched oligonucleotide **2a** (■) and trinucleoside monophosphate **1** (dashed line); $T = 25°C$, $I(NaNO_3) = 1.0$ mol L^{-1}.

(11:4:7:8), the reaction proceeds approximately as rapidly by P-O5′ (Route A) and P-O3′ (Route B) bond cleavage. Over a wide range from pH 2 to 5, the overall reaction is pH-independent and a largely similar product distribution is observed as with the hydronium ion catalyzed cleavage. At pH > 6, the overall reaction is first-order in [HO^-]. Only the P-O3′ cleavage products (**8** and **9**) can be detected, indicating that the P-O3′ cleavage (Route B) predominates under alkaline conditions, as with **1**. Rate constants for the hydronium ion–catalyzed, pH-independent, and hydroxide ion–catalyzed cleavage, k_{cl}^{H}, k_{cl}^{W}, and k_{cl}^{OH}, were obtained by fitting the observed pseudo first-order rate constants, k_{cl}^{obs}, to Eq. (1) by a nonlinear least-squares method. The calculated rate constants, together with those previously obtained for **1**, are presented in Table 1.

$$k_{cl}^{obs} = k_{cl}^{H} a_{H^+} + k_{cl}^{W} + \frac{k_{cl}^{OH} K_W}{a_{H^+}} \quad (1)$$

The rate constants for the hydronium ion–catalyzed and pH-independent cleavage are largely similar with **2a** and **1**, suggesting that the

TABLE 1 Rate Constants for the Partial Reactions of Cleavage of the Phosphate-Branched Oligonucleotide **2a** and the Trinucleoside Monophosphate **1**

	$k_{cl}^{H}/10^{-3}$ L mol^{-1} s^{-1}	$k_{cl}^{W}/10^{-5}$ s^{-1}	$k_{cl}^{OH}/10^{3}$ Lmol^{-1} s^{-1}
2a	3.9 ± 0.5	6 ± 3	0.62 ± 0.06
1	1.6 ± 0.3	9.0 ± 0.9	7.5 ± 0.9

short oligonucleotide arms play no major role under acidic conditions. Hydroxide ion–catalyzed cleavage of **2a**, however, is 12 times slower than the respective reaction of **1**. For comparison, hydroxide ion–catalyzed cleavage of an individual phosphodiester linkage within poly(U) is as rapid as the respective reaction of UpU.[10] Accordingly, the increasing number of negatively charged phosphodiester bonds is not as such a sufficient explanation for the observed retardation of hydroxide ion–catalyzed cleavage. In any case, it seems, on the basis of these results, that even short oligonucleotide chains with no tendency to fold into specific tertiary structures may significantly alter the rate of cleavage of ribonucleoside phosphotriester linkages. In the case of a more complex structure, such as RNA X, the stabilization may be even more marked, possibly sufficient to make RNA X a species that can actually be detected under physiological conditions. The present data additionally serves as a necessary background for further studies with phosphate-branched oligonucleotides, the arms of which may have specific interactions with one another.

REFERENCES

1. Valadkhan, S.; Manley, J.L. Characterization of the catalytic activity of U2 and U6 snRNAs. RNA, **2003**, 9, 892–904.
2. Valadkhan, S.; Manley, J.L. Splicing-related catalysis by protein-free snRNAs. Nature **2001**, 413, 701–707.
3. Massenet, S.; Mougin, A.; Branlant, C. *In* The Modification and Editing of RNA: Posttranscriptional modifications in the U small nuclear RNAs. Grosjean, H.; Benne, R., Eds.; ASM Press: Washington, DC, **1998**, 201.
4. Lönnberg, T.; Kiiski, J.; Mikkola, S. Hydrolytic stability of 2′,3′-*O*-methyleneadenos-5′-yl 2′,5′-di-*O*-methylurid-3′-yl 5′-*O*-methylurid-3′(2′)-yl phosphate: implications to feasibility of existence of phosphate-branched RNA under physiological conditions. Org. Biomol. Chem. **2005**, 3, 1089–1096.
5. Lönnberg, T.; Mikkola, S. Hydrolysis of 2′,3′-*O*-methyleneadenos-5′-yl bis(2′,5′-di-*O*-methylurid-3′-yl) phosphate, a sugar *O*-alkylated trinucleoside 3′,3′,5′-monophosphate: implications for the mechanism of large ribozymes. J. Org. Chem. **2004**, 69, 802–810.
6. Corbridge, D.E.C. Phosphorus—An outline of Its Chemistry, Biochemistry and Technology. Elsevier: Amsterdam, **1990**; 997–999.
7. Mikkola, S.; Kaukinen, U.; Lönnberg, H. The Effect of secondary structure on cleavage of the phosphodiester bonds of RNA. Cell Biochem. Biophys. **2001**, 34, 95–119.
8. Lönnberg, T.; Korhonen, J. Hydrolysis of 2′,3′-*O*-methyleneadenosin-5′-yl bis-5′-*O*-methyluridin-3′-yl phosphate: the 2′-hydroxy group stabilizes the phosphorane intermediate, not the departing 3′-oxyanion, by hydrogen bonding. J. Am. Chem. Soc. **2005**, 127, 7752–7758.
9. Roy, S.K.; Tang, J.-Y. Efficient large scale synthesis of 2′-*O*-alkyl pyrimidine ribonucleosides. Org. Process Res. Dev. **2000**, 4, 170–171.
10. Kuusela, S.; Lönnberg, H. Hydrolysis and isomerization of the internucleosidic phosphodiester bonds of polyuridylic acid: kinetics and mechanism. J. Chem. Soc., Perkin Trans. **1994**, 2, 2109–2113.